Using Mean Field Theory to Guide Biofunctional Materials Design

Uwe Freudenberg, Jens-Uwe Sommer, Kandice R. Levental, Petra B. Welzel, Andrea Zieris, Karolina Chwalek, Katja Schneider, Silvana Prokoph, Marina Prewitz, Ron Dockhorn, and Carsten Werner**

Cell-instructive characteristics of extracellular matrices (ECM) resulting from a subtle balance of biomolecular and biophysical signals must be recapitulated in engineered biomaterials to facilitate regenerative therapies. However, no material explored so far allows the independent tuning of the involved molecular and physical cues due to the inherent correlation between biopolymer concentration and material properties. Addressing the resulting challenge, a rational design strategy for ECM-inspired biohybrid hydrogels based on multi-armed poly(ethylene glycol) and heparin, adapting a mean field approach to identify conditions at which the balance of elastic, electrostatic, and excluded volume forces results in constant heparin concentrations within swollen polymer networks with gradually varied physical properties is introduced. Applying heparin-based biofunctionalization schemes, multiple distinct combinations of matrix parameters could be identified to effectively stimulate the pro-angiogenic state of human endothelial cells and the differentiation of human mesenchymal stem cells. The study demonstrates the power of joint theoretical and experimental efforts in creating bioactive materials with specifically and independently controllable characteristics.

1. Introduction

Biomaterials that mimic extracellular matrices (ECM), and thereby enable control over cell fate decisions through exogenous signals, are vital for regenerative therapies.[1] Recent research has revealed that, together with the provision of morphogens and the presentation of adhesion ligands,[2] the mechanical characteristics of extracellular matrices have a decisive influence on cell fate, provoking the development of materials with effective physical properties.[3] This interplay of biomolecular and biophysical signals thus defines an obvious, but until now unmet, need for a new generation of biomaterials that can be selectively and independently tuned for biomolecular properties and physical material parameters. A conceptual basis to address this need is currently missing. As such, we have developed a rational design approach relying on mean field concepts to guide the design of biofunctional matrices. Considering the decisive role of electrostatic interactions in functional assemblies of living matter we selected a system that allows for a far-reaching modulation of structure-determining forces: crosslinking a hydrophilic and flexible, multi-armed polymer (with four-armed, amino-terminated poly(ethylene glycol) (starPEG) as an example system known for its anti-adhesive characteristics towards proteins,[4] with a multifunctional, highly charged crosslinker (such as heparin (HEP) or a similarly charged glycosaminoglycan), which can function as a multivalent binding site capable of complexing a plethora of important bioactive molecules.[5] We explored whether and how the combination of the particular gel components permits varying the physical and biomolecular characteristics of the swollen materials independently.

Based on the successful experimental verification of the theoretical predictions and the functionalization of starPEG-heparin gels with adhesive ligand peptides (such as the integrin-binding arginine-glycine-aspartic acid sequence (RGD))) and morphogens (vascular endothelial growth factor (VEGF), bone morphogenetic protein-2 (BMP-2)) through covalent and non-covalent conjugation schemes we were able to illustrate the resulting options for two selected example systems: studying the interplay of matrix elasticity and growth factor presentation in inducing the pro-angiogenic state of human endothelial cells and promoting osteogenic differentiation of human mesenchymal stem cells we identified effective combinations of matrix parameters and demonstrated exciting options for the fully matrix controlled direction of the cells, i.e., removed the

Dr. U. Freudenberg, Dr. K. R. Levental, Dr. P. B. Welzel, A. Zieris, K. Chwalek, K. Schneider, S. Prokoph, M. Prewitz, Prof. C. Werner
Leibniz Institute of Polymer Research Dresden (IPF)
Max Bergmann Center of Biomaterials Dresden (MBC)
Hohe Str. 6, 01069 Dresden, Germany
E-mail: werner@ipfdd.de
Dr. U. Freudenberg, Dr. K. R. Levental, Dr. P. Welzel, A. Zieris, K. Chwalek, K. Schneider, S. Prokoph, M. Prewitz, Prof. C. Werner
Technische Universität Dresden
Center for Regenerative Therapies Dresden (CRTD)
Tatzberg 47 01307 Dresden, Germany
Prof. J.-U. Sommer, R. Dockhorn
Leibniz Institute of Polymer Research Dresden (IPF)
Hohe Str. 6, 01069 Dresden, Germany;
E-mail: sommer@ipfdd.de
Prof. J.-U. Sommer, R. Dockhorn
Technische Universität Dresden
Institute for Theoretical Physics
Zellescher Weg 17, 01069 Dresden, Germany

DOI: 10.1002/adfm.201101868

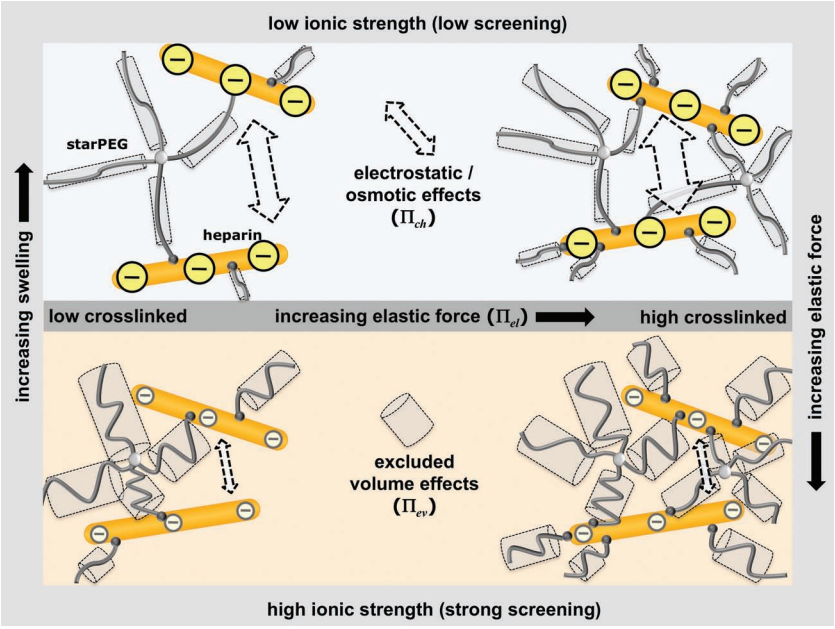

Figure 1. A rational design concept is used to combine star-shaped, end-functionalized poly(ethylene glycol) (starPEG) and heparin in hybrid networks. Schematic representation of the interplay between elastic forces (Π_{el}) (≈crosslinking degree), excluded volume (Π_{ev}), and electrostatic effects (Π_{ch}) maintaining the swelling and heparin concentration of the swollen matrices ($\Pi_{el} = \Pi_{ch} + \Pi_{el}$). Top: electrostatic effects (arrows) dominate the swelling at low salt situations, where the screening is less effective (Debye length ≈ 300 nm); increasing starPEG/heparin ratio γ (≈crosslinking) increases the number of starPEG molecules and therefore the excluded volume effects (cylinders). Bottom: excluded volume effects dominate the swelling at high salt situations, where strong screening occurs (Debye length ≈ 0.2 nm). The interplay of both extension forces (electrostatic and excluded volume) with the varying retraction force (elastic force) is considered within our mean field model of swelling equilibrium to predict swelling and utilize a rational design concept to control hydrogel composition.

need for the supplementation of the fluid media with soluble morphogens.

2. Results

2.1. Mean Field Theory to Explore the Force Balance in Binary Hydrogel Systems

The concentration of the highly charged crosslinker component in the swollen network ($\tilde{c}_{HEP}$) can be assumed to be determined by the interplay of three forces: 1) the elastic ("retraction") force, which is caused by the covalent linkages to the flexible, hydrophilic component; this force is balanced by 2) the excluded volume ("expansion") force, and 3) the electrostatic ("expansion") force (**Figure 1**). Both the elastic retraction and the excluded volume force increase with increasing molar ratio of the gel components (γ). To further explore the impact of these forces on the properties of the gel system in aqueous media it is instructive to consider their contributions as they are affected by the ionic strength. There, the "retraction" force (elastic = Π_{el}) is balanced by either excluded volume (Π_{ev}) or electrostatic (charging = Π_{ch}) effects if high (strong screening of electrical charges, excluded volume effects are pronounced, $\eta = 2.4$) or low salt conditions (low screening of electrical charges, electrostatic interactions are pronounced, $\eta = 20$) are applied, respectively (for details see Figure 1 and Supporting Information).[6] If the elastic force is compensated by the electrostatic interactions only (low salt conditions), i.e.,

$$\Pi_{el} = \Pi_{ch} \quad (1)$$

the concentration of the highly charged crosslinker follows as

$$\tilde{c}_{HEP} \approx \left(1 - \frac{\gamma_c}{\gamma}\right)^{3/2} \gamma^{1/2} \quad (2)$$

where γ_c denotes the molar ratio of the components defining the gelation threshold (γ_c = 0.7, see Figure 1 and Supporting Information). Thus, the concentration of the highly charged crosslinker in the swollen gel was concluded to be a monotonously increasing function of γ (see **Figure 2**a,d). If the excluded volume effects compensate for the elastic force (high salt conditions), i.e.,

$$\Pi_{el} = \Pi_{ev} \quad (3)$$

the concentration of the charged crosslinker is given by

$$\tilde{c}_{HEP} \approx \frac{\delta}{\gamma}\left(1 - \frac{\gamma_c}{\gamma}\right)^{3/5} \quad (4)$$

where δ is the ratio of the molar volumes (of e.g., heparin/starPEG). This function is non-monotonous and increases at low values of γ, while it decreases for larger values of γ (see Figure 2b,d). At physiological salt conditions (phosphate buffered saline (PBS)), these two opposing trends can be taken into account by a numerical solution of the equilibrium condition $\Pi_{el} = \Pi_{ch} + \Pi_{ev}$ ($\eta = 4.2$, see Supporting Information). In fact, our analysis revealed that the interplay of the two combined expansion forces and the elastic (retraction) force (Figure 2d) results in a nearly constant concentration of the highly charged crosslinker (e.g., heparin) in the swollen gels at physiological salt conditions over a wide range of γ (see Figure 2c,d). It is important to note that this desired behavior results from the combination of a highly charged crosslinker and a hydrophilic, flexible but uncharged polymer component, i.e., the combination of electrostatic and excluded volume repulsion. However, localization of the different repulsive forces is required to produce this unique effect and polymer network systems of evenly distributed ionizable moieties cannot be adjusted to produce a similar behavior. The elaborated concept permits one to predict the behavior of gel materials formed from various different building blocks: hydrogels made of starPEG with higher molecular weight or heparin with lower molecular weight were shown to similarly contain nearly constant heparin concentrations at physiological ionic strength (see Supporting

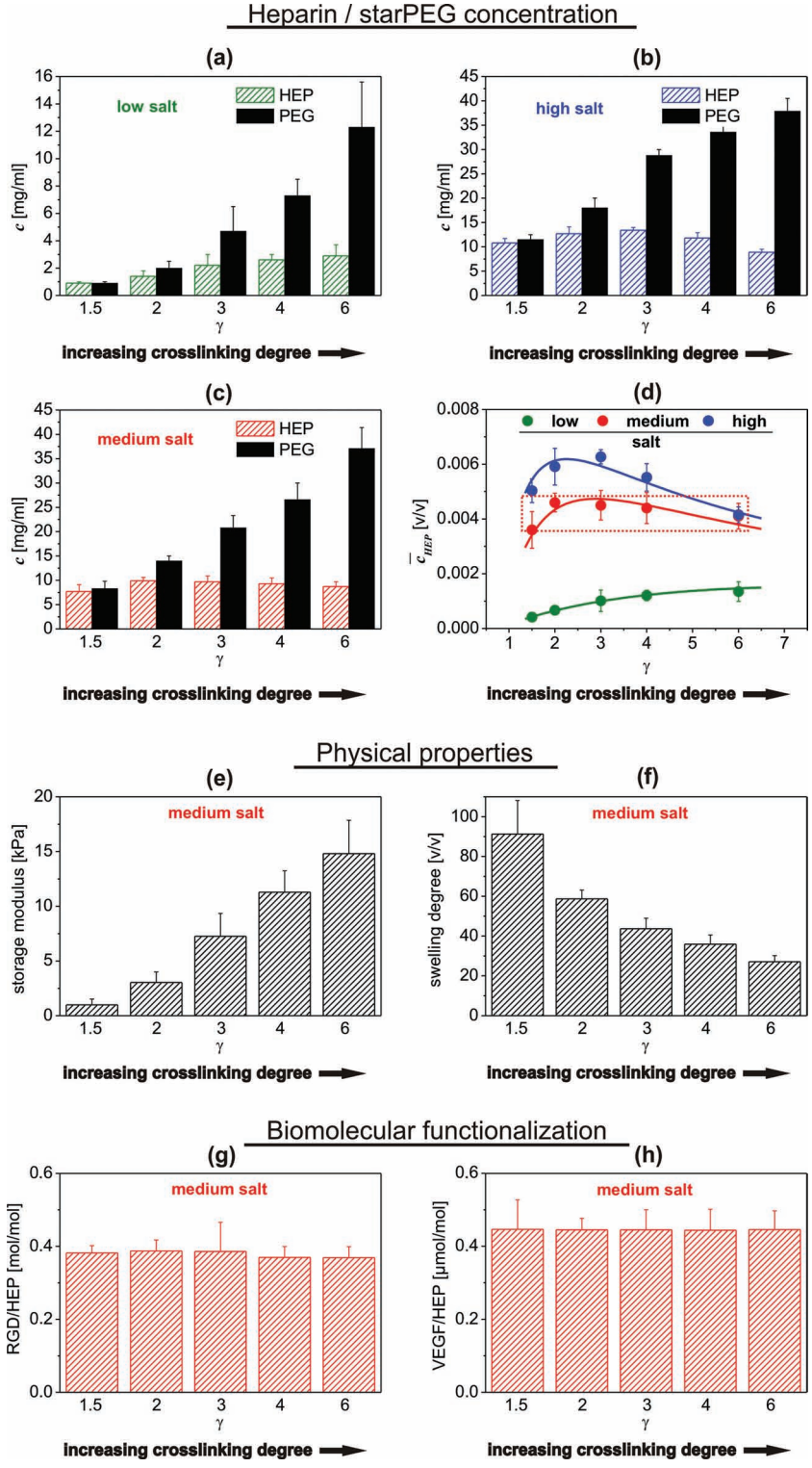

Figure 2. Hydrogel properties vs. starPEG/heparin ratio (γ). a–c) Concentration of heparin and starPEG in the equilibrium swollen state (in mg mL^{-1}) under a) low salt conditions (electrostatic interactions dominate), b) high salt conditions (excluded volume effects dominate), and c) physiological salt conditions (PBS), which results in nearly constant heparin concentration for a wide range of γ. d) Comparison of the volume fraction of heparin (in v/v) in the equilibrium swollen state (see Experimental Section), derived from experimental data (dots) and the mean field approach (lines, see Supporting Information) using $\gamma_c = 0.7$ and $Q_0 = 25$ (see Supporting Information). e) Storage modulus at physiological salt conditions shows that the mechanical properties of the hydrogel are adjustable over a large range by varying γ. f) Degree of swelling at physiological salt conditions. g) Volume concentration of the adhesion ligand RGD covalently immobilized within the hydrogel at physiological salt conditions (PBS). h) Volume concentration of the growth factor VEGF immobilized to heparin within the gel at physiological salt conditions; immobilized amounts of RGD and VEGF correlate well to the heparin concentration at physiological salt conditions [see (c,g, and h)]. The data give mean values and standard deviations based on a minimum of three repeats.

Information Figure 1). Since the level of the heparin concentration depends on the dimension of the building blocks, variation of the heparin levels can be achieved as well.

2.2. starPEG-Heparin Gels with Decoupled Biomolecular and Physical Characteristics

Experimental studies of the exemplarily investigated starPEG-heparin system thoroughly confirmed constant heparin levels of PBS-swollen gels with varying physical properties (see Figure 2c,e,f), validating the rational design strategy described above. Storage moduli ranging from soft (≈500 Pa) to stiff (≈15 kPa) (see Figure 2e) were successfully produced by increasing γ. This allows the adaptation of the gel matrices to the physical conditions of soft and hard tissues ranging in elasticity from brain to osteoid-like bone tissue at a nearly invariant heparin concentration.[7]

Heparin, with its uniquely high affinity to various signaling molecules,[5] was used for the subsequent biomolecular functionalization of the gels. We experimentally determined the binding of vascular endothelial growth factor (VEGF) to materials with varying γ in physiological electrolyte solutions. As expected, the amount of VEGF, when conjugated to the PBS-swollen gels under similar conditions, was equal across the range of γ and thus faithful to the heparin concentration of the swollen matrices (see Figure 2h). Furthermore, the similar release characteristics of three different gel types (γ = 1.5, 3, and 6, see Supporting Information Figure 2) demonstrated that VEGF upload and release are not affected by the degree of crosslinking of the network, which is in line with the estimated mesh size and the protein dimensions.[8] Binding and release of BMP-2 was found to be similarly independent of the network characteristics (γ = 1.5, 3, and 6, see Supporting Information Figure 2). Thus, the hydrogel matrix allows for the customized uploading and long-term delivery of heparin-binding factors, such as VEGF and BMP-2.

In addition to tuning the delivery of morphogens, the control of adhesiveness is crucial in controlling cell fate decisions.[9,10] The covalent conjugation of adhesion ligands similarly showed an excellent correlation of the degree of functionalization with the heparin concentration (≈0.5 mol RGD per mol heparin (see Figure 2g)). As larger molecules are restricted from entering the network[8] and the repellent character of PEG prevents non-specific protein adsorption, the cell adhesivity of our gels can be tuned from "non-adhesive" towards an optimized ligand density for different applications.[10]

Adjusting different heparin concentrations in the gels through the choice of the building blocks offers an additional, effective means for fine-tuning the heparin-based biofunctionalization of the hydrogel materials (see Supporting Information Figure 1).

2.3. Modulation of starPEG-Heparin Hydrogels to Trigger Cell Fate Decisions In Vitro

To illustrate the applicability of the hydrogel system for dissecting distinct signaling mechanisms in cell fate decisions, we created different sets of customized materials to direct primary human endothelial cells (isolated from the umbilical vein, human umbilical vein endothelial cells (HUVECs)) morphogenesis and primary human mesenchymal stem cells (MSCs) differentiation in culture experiments.

Angiogenesis, the formation of new capillary blood vessels, is a key process required for the proper integration of almost any engineered tissue construct and desired in the therapeutic augmentation of wound healing and functional reconstitution. As the various tissues of interest exhibit a myriad of biochemical and biophysical properties (e.g., different stiffness, ECM composition, growth factor environment,[11]) it is important to develop materials capable of effectively stimulating angiogenesis in a multitude of environments. Endothelial cells were shown to migrate and form networks of loosely associated cellular structures in vitro before undergoing tube formation.[9] Here, we utilized starPEG-heparin hydrogels to identify combinations of biophysical and biochemical matrix properties that best promoted morphological changes of endothelial cells being indicative of a capillary-like network formation.[12] We found that the morphology of the endothelial cells is significantly dependent on both the degree of biofunctionality and the mechanical properties of the hydrogels. On soft and intermediate elastic hydrogels (γ = 1.5 and 3) functionalized with VEGF, HUVECs preferentially migrated and elongated to form a network of tube-like structures on less adhesive gels (functionalized with low RGD concentrations; **Figure 3**c, quantified as a significant increase in the aspect ratio of the cell shapes[13] and highlighted with arrows), whereas on more adhesive gels, cell spreading and the formation of a monolayer occurred. In contrast, HUVECs plated on stiffer hydrogels (γ = 6) required a higher RGD concentration (solution concentration applied for conjugation = 20 μg mL^{-1}) to allow adequate cell attachment and tube-like structure formation (Figure 3c). In all cases, presentation of VEGF through the hydrogels resulted in a higher aspect ratio of the cell shapes (e.g., a morphology indicating elongation and network formation of the cells) as compared to the hydrogels without any growth factor incorporation (Figure 3c). These results illustrate, that the gradual and independent variation of synergistically acting matrix characteristics produce multiple sets of effective combinations (panels in Figure 3c, highlighted in blue). Thus, our approach provides customized materials that can be tuned to fit a distinct environment allowing one to promote pro-angiogenic response within different tissues.

To further illustrate the potential of precisely tuned biomaterials for directing a desired cell behavior, we utilized starPEG-heparin hydrogels as a culture carrier system to promote human MSC differentiation. As recent research has shown, MSCs can differentiate in vitro into several anchorage-dependent lineages, including adipogenic, myogenic, and osteogenic, when given the appropriate soluble and insoluble cues.[14,15]

Capitalizing on the affinity of various growth factors to heparin, we sought to determine whether starPEG-heparin hydrogels could deliver the heparin-binding cytokine bone morphogenetic protein-2 (BMP-2) to MSCs to promote osteogenesis. In parallel, by tuning the matrix stiffness independently of the growth factor and RGD concentration, we intended to

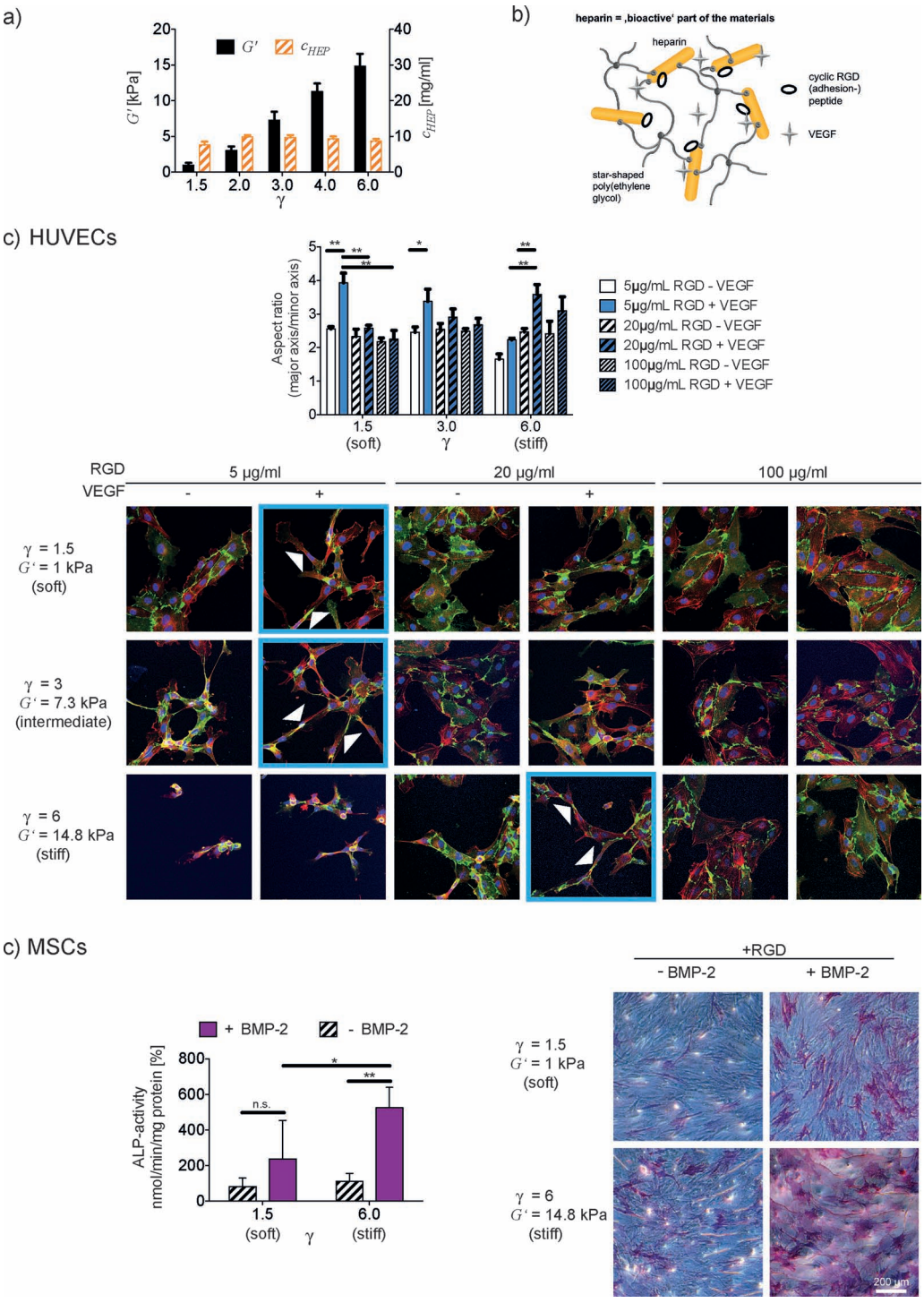

Figure 3. a) Independent tuning of mechanical (indicated by the storage modulus) and biochemical (indicated by the constant heparin concentration) properties with varying γ. b) Heparin is the bioactive component of the hydrogel material mediating cell adhesion and provision of growth factors. c) HUVECs elongate to form a network of tube-like structures (arrows indicate cells with a high aspect ratio as a representative example) on starPEG-heparin hydrogels with independently varying VEGF and RGD incorporation and storage modulus. Images shown are confocal immunofluorescence images of CD31 (green, endothelial cell marker), actin (red), and DAPI (blue) of HUVECs plated for 20–24 h and are representative of results from 3 independent experiments. Mean values and standard error of the mean of three experiments in which >20 cells each is shown (* $p < 0.05$ (significant), ** $p < 0.01$ (highly significant), p is the p-value of probability). d) Stiff, BMP-2 loaded hydrogels promote osteogenic differentiation to a greater extend than softer BMP-2 loaded hydrogels. Left:% of ALP activity of MSCs cultivated on RGD-modified soft ($\gamma = 1.5$) and stiff ($\gamma = 6$) hydrogels functionalized with and without BMP-2 are shown. Mean values and standard deviation of $n = 4$ donors normalized to MSCs cultivated on tissue culture plastic are shown (* $p < 0.05$, ** $p < 0.01$). Right: Representative images of ALP-stained MSCs cultivated on RGD-modified hydrogels further functionalized with and without BMP-2 are shown. ALP is shown in red.

verify that the stiffer hydrogels would be more likely to promote osteogenic differentiation than the softer hydrogels.

Indeed, we found that BMP-2 presented through the hydrogels significantly stimulated alkaline phosphatase (ALP) activity in cells plated on stiff materials (Tukey-Kramer-test: $\gamma = 6 \pm$ BMP: $p < 0.01$, see Figure 3d). Furthermore, cells plated on stiffer materials ($\gamma = 6$) showed enhanced ALP activity in response to matrix-delivered BMP-2 as compared to the soft hydrogels ($\gamma = 1.5$, Tukey-Kramer-test: $p < 0.05$, see Figure 3d), thus illustrating the relevance of both the biomolecular signaling and the physical environment in promoting osteogenic differentiation.

To the best of our knowledge, this is the first system allowing for the combined but independently tunable stimulation of MSCs through matrix elasticity and matrix-presentation of growth factors. As such, this system is highly amenable to become adapted to the needs of a range of related studies by applying different biomolecular functionalization schemes of the gels.

3. Discussion

The reported design strategy of biohybrid networks offers a powerful approach to multifunctional materials with precisely and independently tuned properties. Adapting concepts from theoretical polymer physics to describe the force balance in swollen binary polymer networks allowed us to design a particular set of starPEG-heparin hydrogels for which the volume concentration of heparin remains invariant under physiological conditions over a large range of crosslinking degrees and elastic polymer volume fractions. Experimental studies confirmed that a defined heparin concentration is kept nearly constant in swollen starPEG-heparin gels across a broad range of physical properties. Secondary biomolecular functionalization of the gels, including the association of growth factors and covalent conjugation of adhesive peptides, was found to correlate with the constant heparin level, thus demonstrating that biomolecular functionalization and physical characteristics of the gel materials are independently tunable across a range of relevant parameters. The mechanical properties of the materials can be closely matched to the physical conditions of entirely different tissues, ranging in elasticity from brain to osteoid tissue[7] while providing long-term delivery of critically important growth factors such as VEGF and BMP-2.

Applying these modular matrices with decoupled properties we were able to show that specific combinations of morphogen release, cell adhesive characteristics and elastic properties can be effective in modulating cell fate decisions towards a therapeutically relevant phenotype. Specifically, functionalization of differently crosslinked starPEG-heparin gels with adhesive (RGD) ligand peptides and morphogens (VEGF, BMP-2) through covalent and non-covalent conjugation schemes was demonstrated to induce morphogenesis of human endothelial cells and promote the osteogenic differentiation of human mesenchymal stem cells. For HUVECs, as an example, we were able to tune materials of different stiffness to support pro-angiogenic morphogenesis within a broad range of tissue environments.

4. Conclusions

Using a mean-field-based analysis of the force balance within biohybrid polymer networks we were able to develop a set of starPEG-heparin hydrogels with decoupled physical and biomolecular characteristics. The resulting platform of multibiofunctional materials offers exciting options for the fully matrix controlled direction of the cells, i.e., removes the need for the supplementation of the fluid media with soluble morphogens. Valuable extensions of the introduced gel design result from the incorporation of peptide units to control gel formation (e.g., through coiled-coil interactions) and degradation (through inclusion of matrix metalloproteinase-sensitive peptide sequences),[16] as well as from the selective desulfation of the heparin units to modulate the affinity to various growth factors.[5]

Beyond the particular system investigated, our approach created a road map for the combination of polyelectrolytes with flexible, non-ionic polymer units into networks with decoupled properties. As a proof for this generalizability the theoretical predictions were shown to hold true when varying the molecular weights of the building blocks, resulting in gel materials with similarly decoupled properties but different heparin contents (see Supporting Information Figure 1). This result further extends the options for the formation of hydrogel systems with tailored characteristics.

Biohybrid gels as presented provide a base for thoroughly defined cell culture studies on the interplay of multiple exogenous signals in cellular fate decisions. Beyond that, the novel class of modular gel materials is currently applied in translational research towards regenerative therapies for cardiovascular and neuronal pathologies,[8] diabetes, and other diseases.

5. Experimental Section

Gel Preparation, Characterization and Functionalization: Heparin (MW 14 000, Calbiochem (Merck, Darmstadt, Germany) and a mixture of EDC (Sigma–Aldrich, München, Germany), and *N*-hydroxysulfosuccinimide (sulpho-NHS, Sigma–Aldrich) (2:1 ratio of EDC:sulpho-NHS) were dissolved in deionized, decarbonized water (MilliQ-water) on ice. A twofold molar excess of EDC to amine groups of polyethylene glycol (PEG) was used. After mixing, the heparin and EDC/sulpho-NHS solution was kept on ice (≈2–4 °C) for 15 min to activate the heparin carboxylic acid groups. Amine end-functionalized 4-arm starPEG (MW 10 000, Polymer Source, Inc., Dorval, Canada) was dissolved in MilliQ-water on ice and subsequently added to the activated heparin. The molar ratio of starPEG to heparin was varied from 1.5 to 6. After quickly vortexing, the gels were kept at room temperature for 14 h, followed by excessive washing and swelling in phosphate buffered saline (PBS, Sigma–Aldrich) to remove EDC/sulpho-NHS and unbound starPEG/heparin. The physical properties of the gel materials were characterized using volume swelling and rheometry (see Supporting Information). The gels were chemically modified with RGD-peptides using EDC/sulpho-NHS-activation of heparin and further on VEGF/BMP-2 were non-covalenty conjugated to heparin (see the following sections). All experiments were carried out at least four times unless otherwise indicated.

Volume Swelling Measurements and Calculation of Volume Fraction: The degree of volume swelling Q was calculated as follows: $Q = V/V_0 = (d/d_{reac})^3 V_{reac}/V_0$, where d is the diameter of the swollen gel disk, d_{reac} is the diameter of the unswollen gel disk (cured reaction mixture), V_{reac} is the volume of the cured reaction mixture, and $V_0 = n\nu_{PEG} + n\nu_{HEP}$ is the volume of the dry gel. Experiments were carried out at least four times.

The volume fraction of heparin (see Figure 2d) was calculated according to the following equation: $c_{HEP} = c_{HEP}(m/v)/\rho_{HEP}(m/v)$, where ρ_{HEP} is the density of heparin with 2.14 g mL^{-1}.

Rheological Measurements: Oscillating measurements on the swollen gel disks (PBS) were carried out on a rotational rheometer (ARES LN2, TA Instruments, Eschborn, Germany), fitted with a parallel plate geometry (plate diameter = 25 mm). Frequency sweeps were carried out at 25 °C in a shear frequency range of 10^{-1}–10^{-2} rad s^{-1} with a strain amplitude of 2%.

Modification of the Gels with RGD Peptides: PBS-swollen hydrogels were treated with EDC/sulpho-NHS solution (50 mM EDC and 25 mM sulpho-NHS dissolved in 1/15 M phosphate buffer, 4 °C) to activate the heparin carboxylic acid groups for 45 min followed by flushing in borate buffer (100 mM, pH 8.0, 4 °C). Next, the samples were immersed in cyclo(Arg-Gly-Asp-dTyr-Lys) (RGD) (50 mg mL^{-1}, Peptides International, Louisville, KY, USA) dissolved in borate buffer (100 mM, pH 8.0) for 2 h (room temperature) followed by excessive washing in PBS. Quantification of RGD-peptide in the gels was performed by acidic hydrolysis and subsequent HPLC analysis as described elsewhere.[17]

Uptake and Release of VEGF/BMP-2: Uptake and release of $VEGF_{165}$ (PeproTech GmbH, Hamburg, Germany) or BMP-2 (R&D Systems, Minneapolis, USA) were characterized using enzyme-linked immunosorbent assay (ELISA). Surface-bound gels (n = 3) were placed in custom-made incubation chambers. VEGF solution (200 mL with a concentration of 1 μg mL^{-1}) or BMP-2 (200 mL with a concentration of 1, 2.5 or 6.8 μg mL^{-1}) were added per cm^2. The VEGF or BMP-2 solution was removed, followed by washing with PBS. Each of these solutions was collected and assayed in duplicates using an ELISA Quantikine kit (R&D Systems, Minneapolis, USA). After immobilization using a protein concentration of 1 μg mL^{-1} (for VEGF) or 6.8 μg mL^{-1} (for BMP-2), the growth factors were allowed to release from these gels at 22 °C into 250 μL cm^{-2} of the either serum-free endothelial cell growth medium (for VEGF) or DMEM (for BMP-2). For additional information, the reader is referred to Zieris et al.[18]

Endothelial Cell Culture Experiments: Human endothelial cells from the umbilical cord vein (HUVECs) were collected according to the procedure suggested by Weis et al.[19] 50 000 cells per cm^2 (passage 1 to 4) were seeded onto RGD- and VEGF-functionalized hydrogels in complete ECGM containing 2% calf serum. After 18 h cells were washed, fixed and stained with monoclonal mouse anti-CD31 (BD Bioscience, Heidelberg, Germany) and AlexaFluor 546 goat anti-mouse secondary (Invitrogen) antibodies. Actin was visualised by AlexaFluor 633-labelled Phalloidin (Invitrogen). Confocal images were taken, and ImageJ software[20] was used to quantify the aspect ratio of individual cells as delineated by the actin and CD31 staining similar to that which was published previously.[21] The aspect ratio was determined by calculating the ratio of the major axis of individual cells to their minor axis, with a higher aspect ratio indicating more elongated cells.[13] Aspect ratios are recorded as means ± standard deviation of >20 cells per experiment done in three repeats and statistically analyzed by a two-way analysis of variation test followed by Bonferroni post testing. p values less than 0.05 were considered statistically significant. HUVECs isolated according to the above-mentioned protocol were shown to form tubes on Matrigel (see Supporting Information Figure 3).

Mesenchymal Stem Cell Culture Experiments: Human bone marrow-derived MSCs were isolated from healthy male donors (Caucasians 21–35 years of age). The study was approved by the institutional Review Board of the Medical Faculty at the University Hospital of Technische Universität Dresden. MSCs were expanded and characterized as described previously.[22] In brief, bone marrow mononuclear cells were isolated by Percoll (D = 1.073 g mL^{-1}) density gradient fractionation. For characterization, 1 × 10^6 of these cells were analyzed in a colony forming unit-fibroblast assay. Herein, cells were cultured for 14 days in NH expension medium (MACS Media for non-hematopoietic stem cells, Miltenyi Biotec, Bergisch Gladbach, Germany) and colonies were counted afterwards. Bone marrow derived mononuclear cells were seeded in a plastic tissue culture flask containing Dulbecco's-modified Eagle's medium- low glucose supplemented with 10% fetal bovine serum (DMEM +10% (v/v) FBS) for expansion. After 2 to 3 days non-adherent cells were removed by washing with PBS containing human serum albumin (0.5%) and fresh medium was added.

Adherent cells were cultured until they reached 90% confluence. Cells were then harvested and further characterized by immune staining and flow cytometry analysis (stained positive for CD166, CD105, CD90, and CD73 and negative for CD45, CD34, and CD14) and by osteoblast (ALP activity quantification and von Kossa staining for matrix mineralization) and adipocyte differentiation assays (lipid accumulation was quantified using oil red staining). Based on this characterization the plastic-adherent bone marrow derived mononuclear cell fraction is referred to as mesenchymal stromal cells (MSCs).

MSCs were cultured in DMEM (low glucose) supplemented with FBS (10% (v/v)) and maintained in a humidified atmosphere of CO_2 (5%). For hydrogel experiments, passage 2 MSCs were plated at a density of 15 000 cells cm^{-2} on RGD functionalized starPEG-heparin scaffolds that were preincubated over night with 1.9 μg BMP-2 (R&D Systems) per scaffold. The medium (DMEM +10% (v/v) FBS) was refreshed after 24 h and on day 5 it was changed to serum-free DMEM+supplement containing insulin, transferrin and selenous acid (ITSTM Premix, BD Biosciences). Termination and processing was done on day 7 to determine ALP enzyme activity and to stain for ALP distribution within the culture. Therefore, the cells were washed with PBS and lysed by freezing in H_2O containing Triton X-100 (1% (v/v), Sigma). The cell lysates were incubated with *p*-nitrophenol phosphate and the reaction was monitored at 37 °C for 16 min by measuring the absorbance at a wavelength of 410 nm. The reaction mixture was prepared by adding sodium borate-NaOH (5 mL of 50 mM, pH 9.8) to *p*-nitrophenol phosphate (5 mL of 16 mM) and $MgCl_2$ (20 μL of 1 M). The ALP activity was normalized to the total amount of protein in the lysate by using the macro BCA protein assay (Thermo Scientific) to obtain specific ALP activities. ALP activity data (normalized to controls grown on tissue culture plastic) are recorded as means ± standard deviation of n = 4 donors. Significance was tested applying the Tukey-Kramer multiple comparison test. Additionally, qualitative ALP assessment was performed by processing the samples for histochemical detection based on the manufacturer's protocol (Sigma).

Supporting Information

Supporting Information is available from the Wiley Online Library or from the author.

Acknowledgements

U.F. and J.-U.S contributed contributed equally to this work. The authors thank Roland Vogel for advice on rheometry (Leibniz Institute of Polymer Research Dresden), Martin Bornhäuser and Katrin Müller (University Hospital "Carl Gustav Carus", Technische Universität Dresden, Dresden, Germany) for advice and support on the culture of mesenchymal stem cells, Phillip Seib (Tufts University, Medford, MA, USA), and Ilya Levental (Max Planck Institute for Cell Biology and Genetics, Dresden, Germany) for valuable discussions. U.F. and C.W. were supported by the Deutsche Forschungsgemeinschaft (DFG) through grants WE 2539-7/1, SFB 655 and FOR/EXC999, and by the Leibniz Association. K.R.L., S.P. and C.W. were supported by the Seventh Framework Programme of the European Union through the Integrated Project ANGIOSCAFF. K.S. and C.W. were supported by the Bundesministerium für Bildung, Forschung und Technologie (BMBF) through grant 01 GN 0946.

Received: August 11, 2011
Revised: November 18, 2011
Published online: January 30, 2012

[1] a) M. P. Lutolf, J. A. Hubbell, *Nat. Biotechnol.* **2005**, *23*, 47; b) G. Chan, D. J. Mooney, *Trends Biotechnol.* **2008**, *26*, 382; c) E. S. Place, N. D. Evans, M. M. Stevens, *Nat. Mater.* **2009**, *8*, 457; d) N. Huebsch, D. J. Mooney, *Nature* **2009**, *462*, 426; e) M. P. Lutolf, P. M. Gilbert, H. M. Blau, *Nature* **2009**, *462*, 433; f) D. A. Wang, S. Varghese, B. Sharma, I. Strehin, S. Fermanian, J. Gorham, D. H. Fairbrother, B. Cascio, J. H. Elisseeff, *Nat. Mater.* **2007**, *6*, 385; g) N. Peppas, Z. Hilt, A. Khademhosseini, R. Langer, *Adv. Mater.* **2006**, *18*, 1345.

[2] a) A. M. Kloxin, A. M. Kasko, C. N. Salinas, K. S. Anseth, *Science* **2009**, *324*, 59; b) H. J. Lee, C. Yu, T. Chansakul, N. S. Hwang, S. Varghese, S. M. Yu, J. H. Elisseeff, *Tissue Eng. Part. A* **2008**, *14*, 1843; c) L. Cao, P. R. Arany, Y. S. Wang, D. J. Mooney, *Biomaterials* **2009**, *30*, 4085; d) C. Fischbach, R. Chen, T. Matsumoto, T. Schmelzle, J. S. Brugge, P. J. Polverini, D. J. Mooney, *Nat. Methods* **2007**, *4*, 855; e) T. P. Kraehenbuehl, L. S. Ferreira, P. Zammaretti, J. A. Hubbell, R. Langer, *Biomaterials* **2009**, *30*, 4318; f) S. T. Lee, J. I. Yun, Y. S. Jo, M. Mochizuki, A. J. van der Vlies, S. Kontos, J. E. Ihm, J. M. Lim, J. A. Hubbell, *Biomaterials* **2010**, *31*, 1219; g) E. Fong, D. A. Tirrell, *Adv. Mater.* **2010**, *22*, 5271.

[3] a) D. E. Discher, D. J. Mooney, P. W. Zandstra, *Science* **2009**, *324*, 1673; b) D. E. Discher, P. Janmey, Y. L. Wang, *Science* **2005**, *310*, 1139; c) R. K. Assoian, E. A. Klein, *Trends Cell. Biol.* **2008**, *18*, 347; d) Y.-W. Lin, C.-M. Cheng, P. R. LeDuc, C.-C. Chen, *PLoS ONE* **2009**, *4*, e4293; e) S. Nemir, J. L. West, *Ann. Biomed. Eng.* **2010**, *38*, 2.

[4] a) J. K. Tessmar, A. M. Goepferich, *Macromol. Biosci.* **2007**, *7*, 23; b) N. Peppas, Z. Hilt, A. Khademhosseini, R. Langer, *Adv. Mater.* **2006**, *18*, 1345.

[5] I. Capila, R. J. Linhardt, *Angew. Chem. Int. Ed. Engl.* **2002**, *41*, 391

[6] a) P. J. Flory, J. Rehner, *J. Chem. Phys.* **1943**, *11*, 521; b) H. M. James, E. Guth, *J. Chem. Phys.* **1947**, *15*, 669; c) T. Tanaka, M. Shibayama, A.Onuki, in *Responsive Gels: Volume Transitions I*, (Ed: K. Dusek), Springer, Berlin Heidelberg, Germany **1993**.

[7] a) A. J. Engler, S. Sen, H. L. Sweeney, D. E. Discher, *Cell* **2006**, *126*, 677; b) I. Levental, P. C. Georges, P. A. Janmey, *Soft Matter* **2006**, *3*, 299.

[8] U. Freudenberg, A. Hermann, P. B. Welzel, K. Stirl, S. C. Schwarz, M. Grimmer, A. Zieris, W. Panyanuwat, S. Zschoche, D. Meinhold, A. Storch, C. Werner, *Biomaterials* **2009**, *30*, 5049.

[9] a) D. E. Ingber, J. Folkman, *J. Cell Biol.* **1989**, *109*, 317; b) T. Maciag, J. Kadish, L. Wilkins, M. B. Stemerman, R. Weinstein. *J. Cell Biol.* **1982**, *94*, 511.

[10] a) A. Engler, L. Bacakova, C. Newman, A. Hategan, M. Griffin, D. Discher, *Biophys. J.* **2004**, *86*, 617; b) J. C. Liu, D. A. Tirrell, *Biomacromolecules* **2008**, *9*, 2984.

[11] a) M. P. Lutolf, J. A. Hubbell, *Nat. Biotechnol.* **2005**, *23*, 4; b) M. P. Lutolf, P. M. Gilbert, H. M. Blau, *Nature* **2009**, *462*, 433.

[12] Y. Kubota, H. K. Kleinman, G. R. Martin, T. J. Lawley. *J. Cell Biol.* **1988**, *107*, 1589.

[13] J. P. Califano, C. A. Reinhart-King. *Cell Mol. Bioeng.* **2008**, *1*, 122.

[14] A. J. Engler, S. Sen, H. L. Sweeney, D. E. Discher, *Cell* **2006**, *126*, 677.

[15] a) M. F. Pittenger, A. M. Mackay, S. C. Beck, R. K. Jaiswal, R. Douglas, J. D. Mosca, M. A. Moorman, D. W. Simonetti, S. Craig, D. R. Marshak, *Science* **1999**, *284*, 143; b) R. McBeath, D. M. Pirone, C. M. Nelson, K. Bhadriraju, C. S. Chen, *Dev. Cell* **2004**, *6*, 483; c) A. M. Osyczka, P. S. Leboy, *Endocrinology* **2005**, *146*, 3428.

[16] a) M. Tsurkan, K. R. Levental, U. Freudenberg, C. Werner, *Chem. Commun.* **2010**, *46*, 1141; b) K. Chwalek, K. R. Levental, M. V. Tsurkan, A. Zieris, U. Freudenberg, C. Werner, *Biomaterials* **2011**, *32*, 9649.

[17] K. Salchert, T. Pompe, C. Sperling, C. Werner, *J. Chromatogr. A* **2003**, *1005*, 113.

[18] A. Zieris, S. Prokoph, P. B. Welzel, M. Grimmer, K. R. Levental, W. Panyanuwat, U. Freudenberg, C. Werner, *J. Mater. Sci. Mater. Med.* **2010**, *21*, 914.

[19] J. R. Weis, B. Sun, G. M. Rodgers, *Thromb. Res.* **1991**, *61*, 171.

[20] a) W. S. Rasband, *ImageJ*, U. S. National Institutes of Health, Bethesda, Maryland, USA, http://imagej.nih.gov/ij/, **1997–2011**.

[21] R. Sumagin, C. W. Brown III, I. H. Sarelius, M. R. King, *Ann. Biomed. Eng.* **2008**, *36*, 580.

[22] J. Oswald, S. Boxberger, B. Jorgensen, S. Feldmann, G. Ehninger, M. Bornhauser, C. Werner, *Stem Cells* **2004**, *22*, 377.